

Consequences of Flooding on Spectral Statistics

Arnd Bäcker,^{1,2} Steffen Löck,¹ Normann Mertig,^{1,2} and Torsten Rudolf^{1,2}

¹*Institut für Theoretische Physik, Technische Universität Dresden, 01062 Dresden, Germany*

²*Max-Planck-Institut für Physik komplexer Systeme, Nöthnitzer Straße 38, 01187 Dresden, Germany*

(Dated: November 25, 2018)

We study spectral statistics in systems with a mixed phase space, in which regions of regular and chaotic motion coexist. Increasing their density of states we observe a transition of the level-spacing distribution $P(s)$ from Berry-Robnik to Wigner statistics, although the underlying classical phase-space structure remains unchanged. This transition is induced by flooding, i.e. the disappearance of regular states due to increasing regular-to-chaotic couplings. We account for this effect by a flooding improved Berry-Robnik distribution, in which an effectively reduced size of the regular island enters. To additionally describe power-law level repulsion at small spacings we extend this prediction by explicitly considering the tunneling couplings between regular and chaotic states. This results in a flooding and tunneling improved Berry-Robnik distribution which is in excellent agreement with numerical data.

PACS numbers: 05.45.Mt, 03.65.Sq

I. INTRODUCTION

The universal relation between the statistics of quantum spectra and classical mechanics is a fundamental cornerstone of quantum chaos: For systems with regular dynamics it was conjectured that spectral statistics show Poissonian behavior [1]. In contrast, systems with chaotic dynamics should be described by random matrix theory [2, 3], which can be explained in terms of periodic orbits [4–6]. For generic Hamiltonian systems with a mixed phase space, in which disjoint regions of regular and chaotic motion coexist, universal spacing statistics were obtained by Berry and Robnik [7]. Their derivation is based on the semiclassical eigenfunction hypothesis [8–10], which states that eigenfunctions of a quantum system semiclassically localize on those regions in phase space a typical orbit explores in the long time limit. For regular states in one-dimensional systems this corresponds to the WKB quantization condition [11, 12]

$$\oint_{\mathcal{C}_m} p dq = h_{\text{eff}} \left(m + \frac{1}{2} \right). \quad (1)$$

It shows that the regular state, labeled by the quantum number m , localizes on the quantizing torus \mathcal{C}_m which encloses the area $h_{\text{eff}} (m + \frac{1}{2})$ in phase space. On the other hand the semiclassical eigenfunction hypothesis implies that chaotic states uniformly extend over the chaotic region of phase space. Assuming that the disjoint regular and chaotic regions give rise to statistically uncorrelated level sequences, one obtains the Berry-Robnik level-spacing distribution [7], see Fig. 1 (dash-dotted lines).

The assumption of uncorrelated regular and chaotic level sequences does not hold in the presence of dynamical tunneling [13–26], which quantum mechanically couples regular and chaotic states. If such tunneling couplings are small, regular eigenstates will typically have tiny chaotic admixtures and vice versa. The influence

of such weak couplings on spacing statistics can be described perturbatively [27–31]. Based on this description a tunneling improved Berry-Robnik distribution was de-

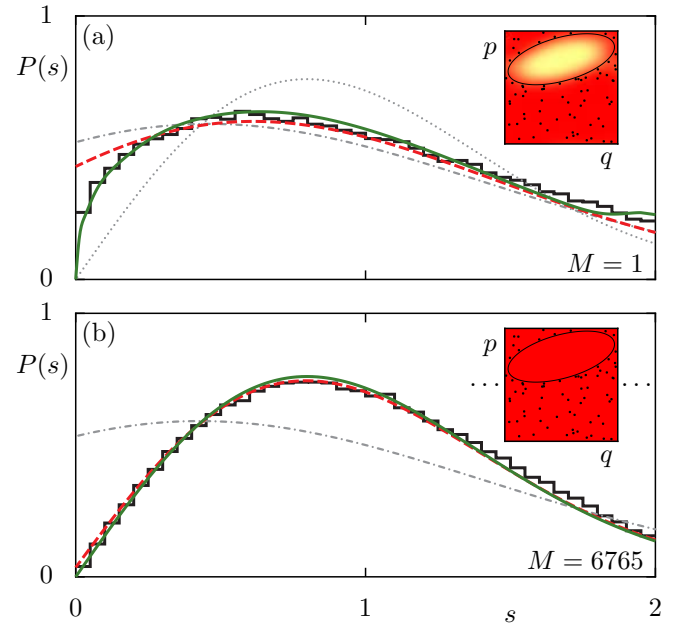


FIG. 1. (Color online) Level-spacing distribution $P(s)$ of the model system, see Sec. II, for $h_{\text{eff}} \approx 1/13$. The numerical data (black histogram) is compared to the flooding improved Berry-Robnik distribution (red dashed lines), Eq. (23), as well as to the flooding and tunneling improved Berry-Robnik distribution (green solid lines), Eq. (29), for system sizes (a) $M = 1$ (weak flooding) and (b) $M = 6765$ (strong flooding); M is introduced in Sec. II A. For comparison the Wigner distribution (dotted lines) and the Berry-Robnik distribution (dash-dotted lines) are shown. The insets show averaged Husimi functions of chaotic eigenstates.

rived recently, which explains the power-law distribution of small spacings in mixed systems [31].

For systems with a large density of states a regular WKB state strongly couples to many chaotic states. As a consequence the corresponding regular eigenstate disappears and chaotic eigenstates penetrate into the regular island, ignoring the semiclassical eigenfunction hypothesis. This effect is called flooding [32–35]. It causes the number N_r^f of regular eigenstates, which actually exist in the regular island to be smaller than the number N_r^{sc} expected from the semiclassical eigenfunction hypothesis. In Refs. [32, 33] it was found that in addition to the WKB quantization condition (1) the regular state on the m th quantizing torus only exists, if

$$\gamma_m < \frac{1}{\tau_{H,c}}. \quad (2)$$

Here, γ_m is the tunneling rate, which describes the initial exponential decay of the m th WKB state to the chaotic region. The Heisenberg time $\tau_{H,c} = h_{\text{eff}}/\Delta_c$ is the ratio of the effective Planck constant h_{eff} and the mean level spacing of the chaotic spectrum Δ_c .

In this paper we study the consequences of flooding on spectral statistics in systems with a mixed phase space. With increasing density of states we observe a transition of the level-spacing distribution from Berry-Robnik, see Fig. 1(a), to Wigner statistics, see Fig. 1(b), although the underlying classical phase-space structure remains unchanged. In order to explain this transition we introduce a flooding improved Berry-Robnik distribution which considers that only $N_r^f \leq N_r^{sc}$ regular states survive in the regular region. We find good agreement with numerical data, see Fig. 1 (red dashed lines). We unify this intuitive prediction with the tunneling improved Berry-Robnik distribution [31], which explicitly considers the tunneling couplings between regular and chaotic states. This results in a tunneling and flooding improved Berry-Robnik distribution, which excellently reproduces the observed transition from Berry-Robnik to Wigner statistics as well as the power-law level repulsion at small spacings, see Fig. 1 (green solid lines).

This paper is organized as follows: In Sec. II we introduce a family of model systems. Their level-spacing distribution is studied in Sec. III, where we demonstrate the transition from Berry-Robnik to Wigner statistics numerically and explain it by the flooding of regular states. We conclude with a summary in Sec. IV.

II. MODEL SYSTEM

In this section we introduce a family of model systems for which the consequences of flooding can be studied in detail.

A. Classical dynamics

We consider systems with a mixed phase space where classically disjoint regions of regular and chaotic motion coexist. As examples we choose one-dimensional kicked systems, described by the classical Hamilton function

$$H(q, p, t) = T(p) + V(q) \sum_{n \in \mathbb{Z}} \delta(t - n), \quad (3)$$

where $T(p)$ is the kinetic energy and the potential $V(q)$ is applied once per kicking period. The dynamics of such systems is determined by the stroboscopic mapping \mathcal{M} of the positions and the momenta (q_n, p_n) at times $t = n$ just after each kick [36],

$$\mathcal{M} : (q_{n+1}, p_{n+1}) = (q_n + T'(p_n), p_n - V'(q_{n+1})). \quad (4)$$

We design the example systems similar to Refs. [21, 23, 32, 37] by the piecewise linear functions

$$t'(p) = \begin{cases} -1 + s_1(p + 1/4), & \text{for } p \in]-1/2, 0[\\ +1 - s_2(p - 1/4), & \text{for } p \in]0, 1/2[, \end{cases} \quad (5)$$

$$v'(q) = -rq - (1 - r)[q + 1/2], \quad (6)$$

where $[x]$ is the floor function and $t'(p)$ is periodically extended. Smoothing the function $t'(p)$ and $v'(q)$ with a Gaussian $G_\epsilon(z) = \exp(-z^2/2\epsilon^2)/\sqrt{2\pi\epsilon^2}$, one obtains analytic functions

$$T'(p) = \int_{-\infty}^{\infty} dz t'(z) G_\epsilon(p - z), \quad (7)$$

$$V'(q) = \int_{-\infty}^{\infty} dz v'(z) G_\epsilon(q - z). \quad (8)$$

By construction these functions have the periodicity properties

$$T'(p + k) = T'(p), \quad (9)$$

$$V'(q + k) = V'(q) - k, \quad (10)$$

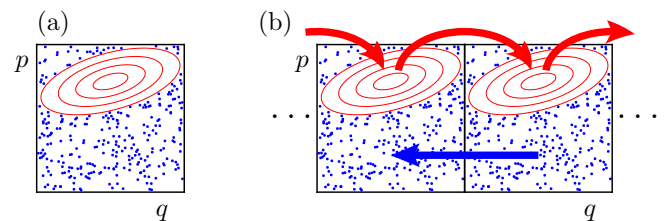


FIG. 2. (Color online) Phase-space portrait of the model system, Eq. (4). For one unit cell $M = 1$ (a) the regular island (red lines) is embedded in the chaotic sea (blue dots). For systems with $M > 1$ (b) the phase space consists of M such unit cells side-by-side. The arrows indicate the transport in the regular islands and in the chaotic sea.

for $k \in \mathbb{Z}$. This allows to consider the map \mathcal{M} on a torus, i.e. $(q, p) \in [-M/2, M/2[\times [-1/2, 1/2[$ with periodic boundary conditions and $M \in \mathbb{N}$. Due to the choice of $T'(p)$ and $V'(q)$, the dynamics is equivalent in each unit cell of phase space with $q \in [k - 1/2, k + 1/2[$ and $k \in \mathbb{Z}$, see Fig. 2. In the following we choose the parameters $s_1 \in [5, 20]$, $s_2 = 2$, $r = 0.46$, and $\epsilon = 0.005$ such that each unit cell has a regular island centered at $(\bar{q}_k, \bar{p}) = (k, 1/4)$. The area of one such island is $A_r \approx 0.32$, which equals the relative size of the regular region in phase space.

Since the islands are transporting to the next unit cell in positive q -direction, i.e. $\mathcal{M}(\bar{q}_k, \bar{p}) = (\bar{q}_{k+1}, \bar{p})$, the center of each island is a fixed point of the M th iterate of the map, $\mathcal{M}^M(\bar{q}_k, \bar{p}) = (\bar{q}_k, \bar{p})$. The surrounding chaotic sea has an average drift in the negative q -direction as the overall transport of the system is zero [38, 39], see Fig. 2. Quantum mechanically this transport suppresses the localization of chaotic eigenstates. In our model systems the hierarchical regions around the regular islands are sufficiently small and also effects of partial transport barriers and nonlinear resonance chains are irrelevant to the numerical studies.

B. Quantization

The quantum system is given by the time-evolution operator over one period of the driving

$$\hat{U} = \exp\left(-\frac{i}{\hbar_{\text{eff}}} V(\hat{q})\right) \exp\left(-\frac{i}{\hbar_{\text{eff}}} T(\hat{p})\right), \quad (11)$$

see, e.g. Refs. [12, 40, 41]. Quantizing the map \mathcal{M} on a two-torus induces the Bloch phases θ_q and θ_p [41, 42] which characterize the quasi-periodicity conditions on the torus. The Bloch phase θ_p is limited by $M(\theta_p + N/2) \in \mathbb{Z}$ because of the periodic boundary conditions, whereas $\theta_q \in [0, 1[$ can be chosen arbitrarily [33, 42].

Due to the quantization on a compact torus the effective Planck constant $\hbar_{\text{eff}} = 2\pi\hbar_{\text{eff}}$ is determined by the number of unit cells M and the dimension of the Hilbert space N

$$\hbar_{\text{eff}} = \frac{M}{N}. \quad (12)$$

Here $N \in \mathbb{N}$ is a free parameter of the quantization and the semiclassical limit is reached for $\hbar_{\text{eff}} \rightarrow 0$. Note that M and N are chosen by continued fractions of $\hbar_{\text{eff}} = 1/(d + \sigma)$ with $\sigma = (\sqrt{5} - 1)/2$ being the golden mean and $d \in \mathbb{N}$. This ensures that $\hbar_{\text{eff}} = M/N$ is as irrational as possible [32]. If M and N were commensurate the quantum system would effectively reduce to less than M cells. In the following we choose $d = 12$ leading to $(M, N) = (1, 13), (21, 265), (610, 7697), (6765, 85361)$, such that the effective Planck constant is approximately fixed at $\hbar_{\text{eff}} \approx 1/13$.

The eigenvalue equation

$$\hat{U} |\phi_n\rangle = e^{i\phi_n} |\phi_n\rangle \quad (13)$$

gives N eigenphases $\phi_n \in [0, 2\pi[$ with corresponding eigenvectors $|\phi_n\rangle$. For fixed \hbar_{eff} it is possible to tune the density of states by varying M and N , i.e. for increasing M, N with constant M/N the density of states rises and flooding becomes more and more prominent, as will be discussed in Sec. III B. In order to numerically solve the eigenvalue equation (13) for $N > 10^4$ we use a band-matrix algorithm, see App. A.

III. SPECTRAL STATISTICS AND FLOODING

In this section we study the influence of flooding on spectral statistics. In Sec. III A we use the model systems introduced in Sec. II to show that flooding leads to a transition of the level-spacing distribution $P(s)$ from Berry-Robnik to Wigner statistics. In Sec. III B we discuss flooding of regular states. Based on this discussion we introduce the flooding improved Berry-Robnik distribution $P_{\text{fi}}(s)$ in Sec. III C, which intuitively explains how the flooding of regular states causes the transition from Berry-Robnik to Wigner statistics. In Sec. III D we unify this prediction with Ref. [31] leading to the more sophisticated flooding and tunneling improved Berry-Robnik distribution $P_{\text{fti}}(s)$. This distribution additionally accounts for the effects of level repulsion between regular and chaotic states. In Sec. III E we discuss three limiting cases in which level repulsion vanishes and spacing statistics are described by the flooding improved Berry-Robnik distribution.

A. Spacing statistics of the model system

We investigate the spectral statistics of the model systems introduced in Sec. II numerically. In order to increase the statistical significance of the spectral data, we perform ensemble averages by varying the parameter s_1 of the map, see Eq. (5). This modifies the chaotic dynamics but leaves the dynamics of the regular region unchanged. Also the Bloch phase θ_q is used for ensemble averaging. For the system sizes $M = 1, 21, 610, 6765$ we choose 50, 50, 10, 4 equidistant values of s_1 in $[5, 20]$ and 400, 19, 10, 1 equidistant values of θ_q in $[0, 1[$, respectively. For each choice the ordered eigenphases ϕ_n give the unfolded level spacings

$$s_n := \frac{N}{2\pi} (\phi_{n+1} - \phi_n). \quad (14)$$

Assuming an uncorrelated superposition of regular and chaotic subspectra corresponding to disjoint regular and chaotic regions in phase space, these spacings are expected to follow the Berry-Robnik distribution [7]. The only relevant parameter of this distribution is the density

of regular states which semiclassically equals the relative size of the regular region in phase space A_r , see Eq. (18). This gives the standard Berry-Robnik distribution

$$P_{\text{BR}}(s) = \frac{d^2}{ds^2} \left\{ \exp(-A_r s) \operatorname{erfc} \left(\frac{\sqrt{\pi}}{2} (1 - A_r) s \right) \right\}. \quad (15)$$

For purely chaotic systems one has $A_r = 0$ such that the Wigner distribution $P_c(s) = (\pi s/2) e^{-\pi s^2/4}$ is recovered. For purely regular systems one has $A_r = 1$ giving the Poisson distribution $P_r(s) = e^{-s}$.

For the model systems introduced in Sec. II one has $A_r \approx 0.32$ such that Eq. (15) predicts the same level-spacing distribution for all system sizes M . This is in contrast to our numerical findings, which show a transition of the level-spacing distribution from Berry-Robnik to Wigner statistics with increasing system size M . In Fig. 3 numerical results for the level-spacing distribution of the model systems are shown as black histograms. For the case of only one unit cell (a) the level-spacing distribution roughly follows the Berry-Robnik distribution (dash-dotted line). Increasing the system size to $M = 21$ unit cells (b) the level-spacing distribution shows global deviations from the Berry-Robnik distribution. For even larger system sizes (c, d) we observe a transition to the Wigner distribution (dotted line). This transition is caused by flooding of regular states, which we discuss in the following section.

B. Flooding of regular states

We now show how the number of regular and chaotic states is modified in the presence of flooding. According to Eq. (1) each regular state occupies an area h_{eff} in phase space. Hence, the maximal number of quantizing tori m_{max} per island is given by

$$m_{\text{max}} = \left\lfloor \frac{A_r}{h_{\text{eff}}} + \frac{1}{2} \right\rfloor \approx \frac{A_r}{h_{\text{eff}}} \quad (16)$$

and the quantum number m runs from 0 to $m_{\text{max}} - 1$. Since we consider a chain of M islands there are M regular levels supported by the m th quantizing tori of the M islands. Hence, we semiclassically expect

$$N_r^{\text{sc}} = m_{\text{max}} M \approx A_r M / h_{\text{eff}} \quad (17)$$

regular states supported by the M regular islands of size A_r . The semiclassically expected density of regular states ρ_r^{sc} is therefore given by the relative size of the regular region,

$$\rho_r^{\text{sc}} := \frac{N_r^{\text{sc}}}{N} \approx A_r. \quad (18)$$

Similarly we expect $N_c^{\text{sc}} = N - N_r^{\text{sc}}$ chaotic states and $\rho_c^{\text{sc}} = 1 - \rho_r^{\text{sc}}$.

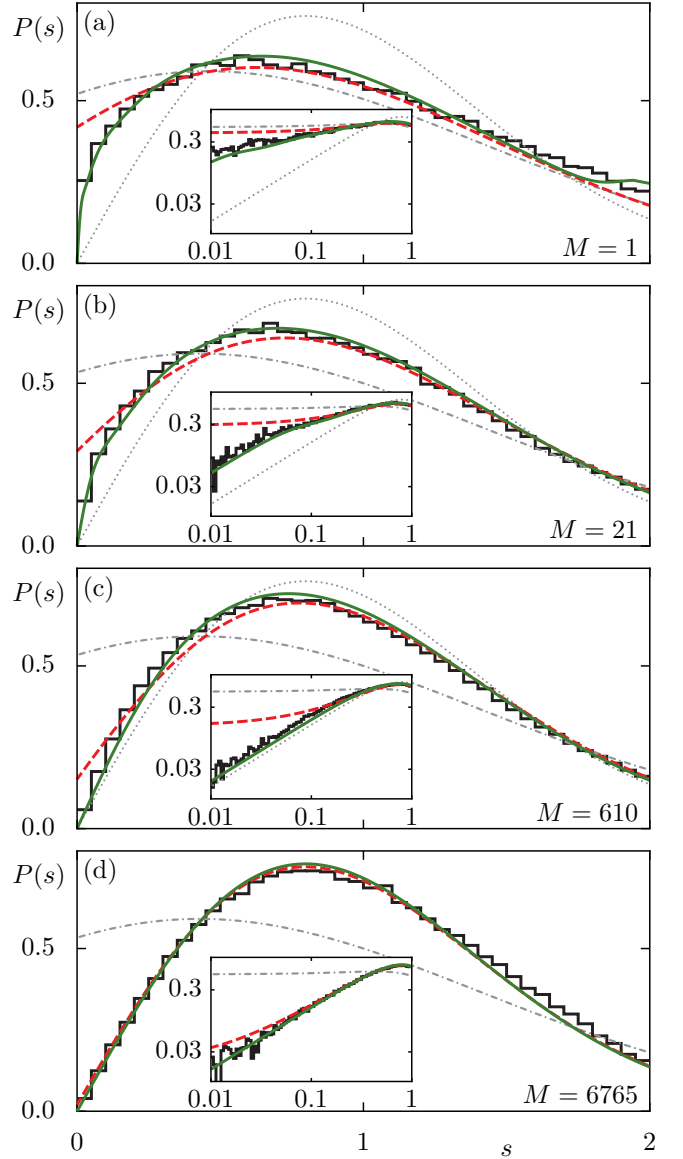


FIG. 3. (Color online) Level-spacing distribution $P(s)$ of the model system for $h_{\text{eff}} \approx 1/13$. The numerical data (black histograms) shows a transition from the Berry-Robnik distribution (dash-dotted lines) to the Wigner distribution (dotted lines) with increasing system size $M = 1, 21, 610$, and 6765 (a-d). This data is compared to the flooding improved Berry-Robnik distribution (red dashed lines), Eq. (23), as well as to the flooding and tunneling improved Berry-Robnik distribution (green solid lines), Eq. (29). The insets show the same distributions on a double logarithmic scale.

Due to dynamical tunneling regular and chaotic states are coupled. The average coupling of the regular states localizing on the m th quantizing tori to the chaotic states is given by the typical coupling v_m [31]. It is determined by the tunneling rate γ_m which describes the initial exponential decay of the m th regular WKB state to the

chaotic sea,

$$v_m = \frac{N}{2\pi} \sqrt{\frac{\gamma_m}{N_c^{\text{sc}}}} = \frac{1}{2\pi} \sqrt{\frac{\gamma_m}{h_{\text{eff}} \rho_c^{\text{sc}}}} \sqrt{M}. \quad (19)$$

We compute the system specific tunneling rates γ_m numerically [23]. They only depend on Planck's constant h_{eff} and the classical phase-space structure of one regular island, which are fixed in our investigations. Hence, the factor $\sqrt{\gamma_m/(h_{\text{eff}} \rho_c^{\text{sc}})}$ in Eq. (19) is constant for our model systems and the typical coupling v_m is tunable by the system size M . Note that the couplings v used in Refs. [32, 33] differ by the factor ρ_c^{sc} from our definition, Eq. (19), due to a different choice of dimensionless units.

In Ref. [32] it was shown that in addition to the WKB quantization condition (1) regular states only exist on the m th quantizing tori, if the tunneling rate γ_m is smaller than the inverse Heisenberg time of the chaotic subsystem, $\gamma_m < 1/\tau_{\text{H},c}$, Eq. (2). Using Eq. (19) and $\tau_{\text{H},c} = h_{\text{eff}}/\Delta_c = N_c^{\text{sc}}$ we rewrite this existence criterion in terms of the typical coupling,

$$v_m < \frac{1}{2\pi \rho_c^{\text{sc}}}. \quad (20)$$

If the existence criterion (20) is fulfilled, the typical coupling of the WKB states on the m th quantizing tori is smaller than the chaotic mean level spacing and the corresponding regular eigenstates exist. If v_m increases beyond this threshold, the regular states on the m th quantizing tori effectively couple to an increasing number of spectrally close chaotic states. Consequently the corresponding regular eigenstates disappear. This process is called flooding of regular states [32, 33, 43, 44]. Thus for large typical couplings v_m the number N_r^f of regular states which actually exist in the regular islands is smaller than the semiclassically expected number N_r^{sc} of regular states. The quantizing tori of the $N_r^{\text{sc}} - N_r^f$ regular states which violate Eq. (20) are flooded by chaotic states in phase space. Note that for our model systems the relation $v_0 < v_1 < v_2 < \dots$ holds, such that the quantizing tori are flooded in the order of decreasing quantum number m from the border to the center of the regular islands.

C. Flooding improved Berry-Robnik distribution

We now introduce a flooding improved Berry-Robnik distribution which takes the flooding of regular states into account. For that purpose we compute the density of regular states ρ_r^f in the presence of flooding. Starting from the semiclassically expected density of regular states, Eq. (18), and using Eqs. (12) and (17) we obtain

$$\rho_r^{\text{sc}} \approx \sum_{m=0}^{m_{\text{max}}-1} h_{\text{eff}}. \quad (21)$$

This expression shows that each quantizing torus semiclassically contributes one Planck cell to the density of

states. To compute the density of regular states ρ_r^f in the presence of flooding we include only those quantizing tori in the sum in Eq. (21), for which the existence criterion (20) holds, and obtain [32, 33]

$$\rho_r^f := \sum_{m=0}^{m_{\text{max}}-1} h_{\text{eff}} \left[1 - \Theta \left(v_m - \frac{1}{2\pi \rho_c^{\text{sc}}} \right) \right]. \quad (22)$$

In Fig. 4 the density of regular states ρ_r^f is shown for the example system at $h_{\text{eff}} \approx 1/13$ versus the system size M on a logarithmic abscissa. It decreases with increasing system size M and has a step whenever a typical coupling v_m equals $1/(2\pi \rho_c^{\text{sc}})$. The semiclassical density of regular states ρ_r^{sc} is an upper limit. In the spirit of Eq. (18), $\rho_r^{\text{sc}} \approx A_r$, we interpret the density of regular states ρ_r^f in the presence of flooding by an area in phase space. For $M = 1, 21, 610$, and 6765 the insets of Fig. 4 show this area enclosed by a gray torus. In addition the averaged Husimi functions (yellow-red color scale) illustrate that the surviving regular states localize in this area ρ_r^f , which decreases in the flooding limit $M \rightarrow \infty$. Already for the system with one unit cell, $M = 1$, we find that ρ_r^f is smaller than its semiclassical expectation ρ_r^{sc} because the outermost regular state of quantum number $m = 3$ violates the existence criterion (20).

Note that the amount by which a regular state is flooded can also be described by smooth functions, e.g. by the fraction of regular states [33] or the asymptotic flooding weight [44]. However, they do not provide a significant advantage for our investigations.

To obtain a description of the level-spacing distribution which includes flooding, we now use prediction (22) for the density of regular states ρ_r^f instead of the relative

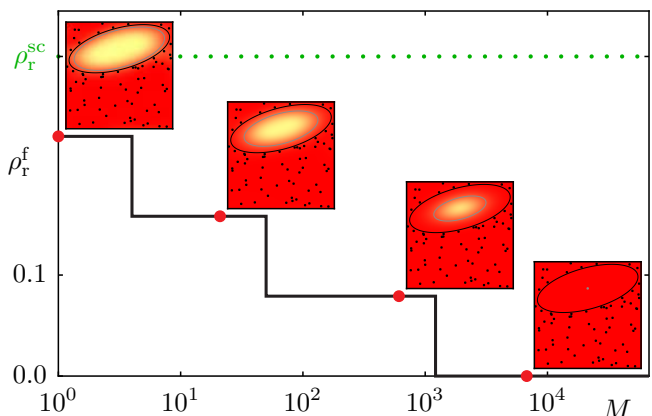


FIG. 4. (Color online) Density of regular states ρ_r^f in the presence of flooding, Eq. (22), vs. the system size M for $h_{\text{eff}} \approx 1/13$ on a logarithmic abscissa. For comparison the semiclassically expected density of regular states ρ_r^{sc} is shown (green dotted line). The insets illustrate the classical phase space where the gray tori enclose the area ρ_r^f for $M = 1, 21, 610$, and 6765 . In addition the averaged Husimi function of all chaotic eigenstates folded into the first unit cell is shown.

size of the regular region A_r as the relevant parameter in Eq. (15). With $\rho_c^f := 1 - \rho_r^f$ this leads to the flooding improved Berry-Robnik distribution

$$P_{\text{fi}}(s) = \frac{d^2}{ds^2} \left\{ \exp(-\rho_r^f s) \operatorname{erfc} \left(\frac{\sqrt{\pi}}{2} \rho_c^f s \right) \right\}, \quad (23)$$

which is our first main result. In Fig. 3 we compare the numerically determined nearest-neighbor level-spacing distribution to the analytical prediction (23) for our model system. With increasing system size M we find a global transition of the level-spacing distribution from Berry-Robnik to Wigner statistics. This global transition is well described by the flooding improved Berry-Robnik distribution, Eq. (23). It is a consequence of flooding, which reduces the density of regular states below its semi-classical expectation, $\rho_r^f \leq \rho_r^{\text{sc}}$. According to Eq. (18) this can be interpreted as a flooding induced decrease of the regular region in phase space. In the limit $M \rightarrow \infty$ the regular islands are completely flooded and no regular state exists. Hence, the Wigner distribution is obtained.

Note that even for the case of only one unit cell, see Fig. 3(a), non-zero couplings v_m exist such that the numerical data is better described by the flooding improved Berry-Robnik distribution, Eq. (23), than by Eq. (15).

At small spacings deviations between numerical data and the flooding improved Berry-Robnik distribution are visible. They occur due to level repulsion between the surviving regular and the chaotic levels, which is not considered within this approach and will be incorporated in the following section.

D. Flooding and tunneling improved Berry-Robnik distribution

We now unify the flooding improved Berry-Robnik distribution, Eq. (23), with the tunneling improved Berry-Robnik distribution [31]. The resulting flooding and tunneling improved Berry-Robnik distribution allows to describe both, the effect of flooding and the power-law level repulsion at small spacings. The derivation is done along the lines of Ref. [31]. We incorporate the effects of flooding into this theory by replacing the number of regular states N_r^{sc} with the number of surviving regular states N_r^f which fulfill the existence criterion (20). The other regular states, which fulfill the WKB quantization condition (1) but have strong couplings to the chaotic sea, $v_m > 1/(2\pi\rho_c^{\text{sc}})$, are assigned to the chaotic subspectrum. Level repulsion is then modeled by accounting for the small tunneling couplings v_m between the N_r^f surviving regular states and the chaotic states perturbatively.

Following Refs. [7, 28, 30, 31] the flooding and tunneling improved Berry-Robnik distribution $P_{\text{fti}}(s)$ consists of three distinct parts

$$P_{\text{fti}}(s) = p_{r-r}(s) + p_{c-c}(s) + p_{r-c}(s). \quad (24)$$

Here $p_{r-r}(s)$ describes the contribution of level spacings between two regular levels, $p_{c-c}(s)$ the contribution of

level spacings between two chaotic levels, and $p_{r-c}(s)$ the contribution of level spacings formed by one regular and one chaotic level in the superposed spectrum. In our model systems the number of quantizing tori m_{max} is small, e.g. $m_{\text{max}} \approx 4$, and the M regular levels with the same quantum number m are equispaced with distance N/M in the unfolded spectrum [45]. Hence, the regular levels do not follow the generic Poissonian behavior occurring for large m_{max} , but are well separated,

$$p_{r-r}(s) \approx 0. \quad (25)$$

Furthermore,

$$p_{c-c}(s) = P_c(s)[1 - \rho_r^{\text{sc}} s], \quad (26)$$

where $P_c(s)$ is the Wigner distribution, which describes the probability to find a spacing s in the chaotic subspectrum. The second factor $[1 - \rho_r^{\text{sc}} s]$ describes the probability to find a gap in the regular subspectrum. For the third term in Eq. (24) one finds [31]

$$p_{r-c}(s) = p_{r-c}^{(0)}(s) \frac{1}{N_r^f} \sum_{m=0}^{N_r^f-1} \frac{\tilde{v}_m}{v_m} X\left(\frac{s}{2v_m}\right), \quad (27)$$

with $X(x) := \sqrt{\pi/2} x \exp(-x^2/4) I_0(x^2/4)$, where I_0 is the zeroth order modified Bessel function and $\tilde{v}_m = v_m / \sqrt{1 - 2\pi(\rho_c^{\text{sc}} v_m)^2}$. The contribution of the zeroth order regular-chaotic spacings, $p_{r-c}^{(0)}(s)$, is given by

$$p_{r-c}^{(0)}(s) = 2\rho_c^{\text{sc}} \rho_r^{\text{sc}} \exp\left(-\frac{\pi(\rho_c^{\text{sc}} s)^2}{4}\right). \quad (28)$$

Using Eqs. (25), (26), and (27) in Eq. (24) we obtain the flooding and tunneling improved Berry-Robnik distribution

$$P_{\text{fti}}(s) = P_c(s)[1 - \rho_r^{\text{sc}} s] + p_{r-c}^{(0)}(s) \frac{1}{N_r^f} \sum_{m=0}^{N_r^f-1} \frac{\tilde{v}_m}{v_m} X\left(\frac{s}{2v_m}\right), \quad (29)$$

which is our final result. In Eq. (29) one has to sum over the $N_r^f \leq N_r^{\text{sc}}$ regular states, which fulfill the existence criterion (20). This selection of the regular states takes flooding into account. In addition power-law level repulsion at small spacings is described by the last term of Eq. (29).

In Fig. 3 we compare the numerical results for the level-spacing distribution to the flooding and tunneling improved Berry-Robnik distribution, Eq. (29) (green solid lines). We find excellent agreement. The global transition of the level-spacing distribution from the Berry-Robnik distribution in Fig. 3(a) for a system with one unit cell to the Wigner distribution in Fig. 3(d) for a system with $M = 6765$ is well described. This transition is caused by the disappearance of regular states due to flooding. Furthermore, the flooding and tunneling improved Berry-Robnik distribution, Eq. (29), reproduces

the power-law level repulsion of $P(s)$ at small spacings, which is caused by small tunneling splittings between the surviving regular and chaotic states. This can be seen particularly well in the double logarithmic insets of Fig. 3.

E. Limiting cases

Depending on the interplay between the flooding limit $M \rightarrow \infty$ and the semiclassical limit $h_{\text{eff}} \rightarrow 0$, we identify three cases, in which the tunneling corrections of Sec. III D are insignificant.

Case (i) is the flooding limit with fixed h_{eff} and $M \rightarrow \infty$ in which all regular states are flooded. Asymptotically one obtains the Wigner distribution, see Fig. 3(d). Note that a further increase of the system size after all regular states have been flooded completely, may lead to the localization of chaotic eigenstates which affects spectral statistics [46, 47].

Case (ii) considers the semiclassical limit, $h_{\text{eff}} \rightarrow 0$, for fixed system sizes M . In this case both flooding and tunneling corrections vanish due to exponentially decreasing tunneling couplings. Hence, the spacing statistics tend towards the standard Berry-Robnik distribution, Eq. (15), [31, 48].

In case (iii) the semiclassical limit $h_{\text{eff}} \rightarrow 0$ and the flooding limit $M \rightarrow \infty$ are coupled such that ρ_r^f is constant and smaller than ρ_r^{sc} . In this limit flooding is present yet the tunneling corrections at small spacings vanish. In this case spacing statistics are given by the flooding improved Berry-Robnik distribution, Eq. (23).

In Fig. 5 we illustrate spectral statistics in the limit of case (iii). We consider the model systems for $(M, N) = (5, 63), (34, 735), (89, 2458), (1597, 77643)$ such that the density of regular states is fixed, $\rho_r^f \approx 0.58\rho_r^{\text{sc}}$, and $h_{\text{eff}} \approx 1/13, 1/22, 1/28, 1/49$ decreases. Both the numerical data and the flooding and tunneling improved Berry-Robnik distribution, Eq. (29), tend towards the flooding improved Berry-Robnik distribution, Eq. (23). The vanishing influence of the tunneling corrections at small spacings is particularly visible in the insets, which show the spacing distributions on a double logarithmic scale.

IV. SUMMARY

In this paper we study the impact of flooding on the level-spacing distribution $P(s)$ for systems with a mixed phase space. Numerically we find a transition from Berry-Robnik to Wigner statistics with increasing density of states. We explain this transition by the flooding of regular islands. It reduces the density of regular states ρ_r^f below its semiclassical expectation ρ_r^{sc} which can be interpreted as a flooding induced decrease of the regular region in phase space. Taking this into account we derive a flooding improved Berry-Robnik distribution,

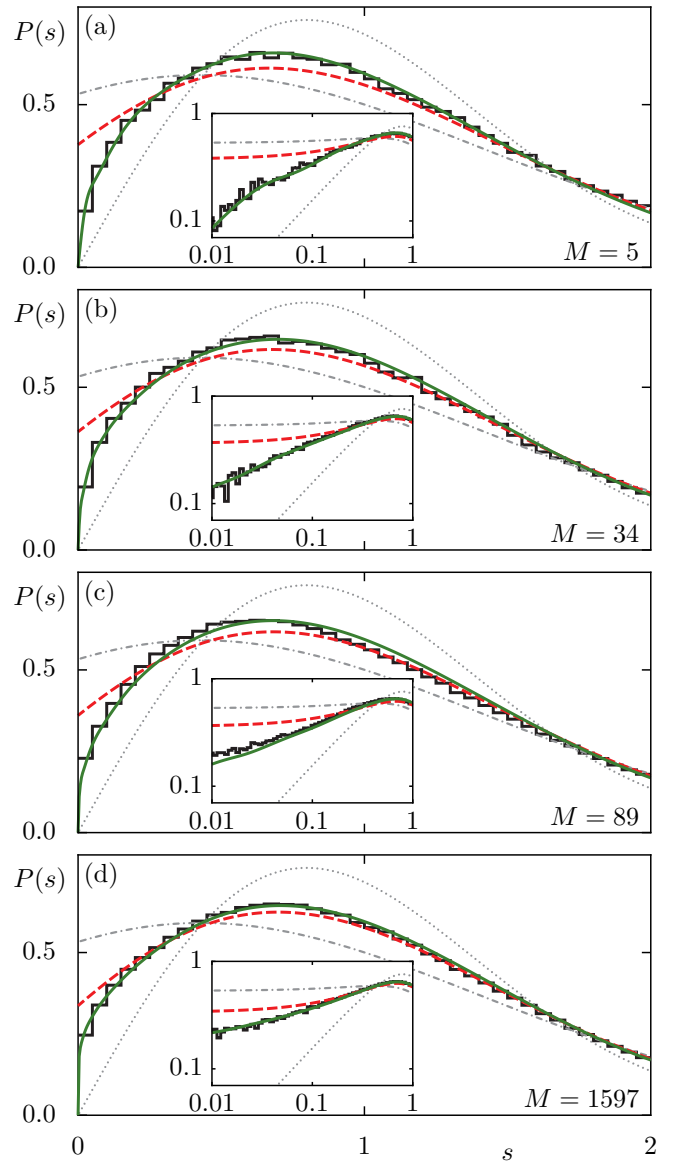


FIG. 5. (Color online) Level-spacing distribution $P(s)$ of the model system at fixed density of regular states $\rho_r^f \approx 0.58\rho_r^{\text{sc}}$. The numerical data (black histograms) is compared to the flooding improved Berry-Robnik distribution (red dashed lines), Eq. (23), as well as to the flooding and tunneling improved Berry-Robnik distribution (green solid lines), Eq. (29), for $(M, N) = (5, 63), (34, 735), (89, 2458),$ and $(1597, 77643)$ (a-d), corresponding to $h_{\text{eff}} \approx 1/13, 1/22, 1/28,$ and $1/49$, respectively. For comparison the Wigner distribution (dotted lines) and the Berry-Robnik distribution (dash-dotted lines) are shown. The insets show the same distributions on a double logarithmic scale.

which reproduces the observed transition of the level-spacing statistics. We unify this prediction with the tunneling improved Berry-Robnik distribution [31] which includes power-law level repulsion. This gives the flooding and tunneling improved Berry-Robnik distribution which

shows excellent agreement with numerical data. We expect that our results can also be applied to systems with more complicated phase-space structures.

ACKNOWLEDGMENTS

We thank Roland Ketzmerick and Lars Bittrich for stimulating discussions. Furthermore, we acknowledge support by the Deutsche Forschungsgemeinschaft within the Forschergruppe 760 “Scattering Systems with Complex Dynamics.”

Appendix A: Periodic band matrix

Our aim is to calculate the eigenphases ϕ_n from Eq. (13) numerically up to Hilbert-space dimension $N \approx 10^5$. This is possible due to a band-matrix algorithm [49] which was used in Refs. [32, 33] and is presented in the following.

We start with the matrix representation of the symmetrized time-evolution operator,

$$\hat{U}^{\text{sym}} = e^{-\frac{i}{2\hbar_{\text{eff}}}T(\hat{p})} e^{-\frac{i}{\hbar_{\text{eff}}}V(\hat{q})} e^{-\frac{i}{2\hbar_{\text{eff}}}T(\hat{p})}, \quad (\text{A1})$$

in the basis of the discretized position states $|q_k\rangle$,

$$U_{k,l}^{\text{sym}} := \langle q_k | \hat{U}^{\text{sym}} | q_l \rangle, \quad (\text{A2})$$

with $q_k = h_{\text{eff}}(k + \theta_p - \frac{1}{2})$ and $k, l = 0, 1, \dots, N-1$. This matrix has dominant contributions around the diagonal and in the upper right and lower left corners, i.e. \hat{U}^{sym} can be approximated by a periodic band matrix. For our model systems the width of the band depends on the extrema of $V'(q)$. The essential step for computing the eigenvalues of U^{sym} is to find a similarity transformation from this periodic band matrix to a band matrix. For the hermitian case a similar idea was used in Ref. [50].

Since the kicking potential is symmetric about $q = 0$ for $M(\theta_p + N/2) \in \mathbb{Z}$, $V(q_l) = V(q_{N-l})$, we find

$$U_{k,l}^{\text{sym}} = U_{N-l, N-k}^{\text{sym}}. \quad (\text{A3})$$

Hence, the set of eigenvectors $|\phi_n\rangle$, for which we choose the phase such that $\langle q_0 | \phi_n \rangle = \langle q_0 | \phi_n \rangle^*$, satisfies

$$\langle q_l | \phi_n \rangle = \langle q_{N-l} | \phi_n \rangle^*, \quad (\text{A4})$$

where the star denotes the complex conjugation and l runs from 1 to $N-1$. Based on these relations it is

possible to find a unitary transformation \hat{A} to a set of purely real vectors $|\psi_n\rangle := \hat{A}|\phi_n\rangle$, given by

$$\langle q_0 | \psi_n \rangle = \langle q_0 | \phi_n \rangle \quad (\text{A5})$$

$$\langle q_{2k-1} | \psi_n \rangle = \frac{1}{\sqrt{2}}(\langle q_k | \phi_n \rangle + \langle q_{N-k} | \phi_n \rangle) \quad (\text{A6})$$

$$\langle q_{2k} | \psi_n \rangle = \frac{1}{i\sqrt{2}}(\langle q_k | \phi_n \rangle - \langle q_{N-k} | \phi_n \rangle) \quad (\text{A7})$$

$$\langle q_{N-1} | \psi_n \rangle = \langle q_{N/2} | \phi_n \rangle. \quad (\text{A8})$$

Here, k runs from 1 to $(N-1)/2$ for odd N or from 1 to $(N-2)/2$ for even N and the last row has to be considered only for even N .

We now define a new operator \hat{W} , given by the unitary transformation of \hat{U}^{sym} with \hat{A} ,

$$\hat{W} := \hat{A} \hat{U}^{\text{sym}} \hat{A}^{-1}. \quad (\text{A9})$$

Its matrix representation W in the basis of position states $|q_k\rangle$ has a banded structure with twice the bandwidth of the matrix U^{sym} but without components in the upper right and lower left corners. Furthermore it is symmetric,

$$W_{k,l} = W_{l,k}, \quad (\text{A10})$$

with complex matrix elements $W_{k,l}$. The unitary transformation (A9) leads to a new eigenvalue problem with the same eigenphases as in Eq. (13),

$$\hat{W} |\psi_n\rangle = e^{i\phi_n} |\psi_n\rangle. \quad (\text{A11})$$

Numerical standard libraries only provide methods for the eigenvalue computation of real symmetric or complex hermitian band matrices but not for unitary band matrices such as W . Hence, we first calculate the real part of the eigenvalues, following from $\text{Re}\{W\} |\psi_n\rangle = \cos \phi_n |\psi_n\rangle$, and afterwards the imaginary part from $\text{Im}\{W\} |\psi_m\rangle = \sin \phi_m |\psi_m\rangle$. This is possible since the eigenvectors $|\psi_n\rangle$ are purely real. From these results one can recover the eigenphases ϕ_n by the requirement $\cos^2 \phi_n + \sin^2 \phi_m = 1$. The corresponding eigenfunctions $|\psi_n\rangle$ can be obtained from Eq. (A11) by the method of inverse iteration using an LU decomposition. By the mapping of the original eigenvalue problem, Eq. (13), to the band matrix form, Eq. (A11), it is possible to compute both eigenvalues and eigenfunctions with a numerical effort scaling like N^2 in contrast to the standard diagonalization procedures which scale like N^3 .

-
- [1] M. V. Berry and M. Tabor, Proc. R. Soc. A **356**, 375 (1977).
 [2] O. Bohigas, M. J. Giannoni, and C. Schmit, Phys. Rev. Lett. **52**, 1 (1984).

- [3] G. Casati, F. Valz-Gris, and I. Guarneri, Lett. Nuovo Cimento **28**, 279 (1980).
 [4] M. V. Berry, Proc. R. Soc. A **400**, 229 (1985).
 [5] M. Sieber and K. Richter, Phys. Scr. **T90**, 128 (2001).

- [6] S. Heusler, S. Müller, A. Altland, P. Braun, and F. Haake, Phys. Rev. Lett. **98**, 044103 (2007).
- [7] M. V. Berry and M. Robnik, J. Phys. A **17**, 2413 (1984).
- [8] I. C. Percival, J. Phys. B **6**, 229 (1973).
- [9] M. V. Berry, J. Phys. A **10**, 2083 (1977).
- [10] A. Voros, in *Stochastic Behavior in Classical and Quantum Hamiltonian Systems*, Lecture Notes in Physics Vol. 93 (Springer-Verlag, Berlin, 1979), pp. 326–333.
- [11] L. D. Landau and E. M. Lifshitz, *Course of Theoretical Physics, Vol. 3: Quantum Mechanics* (Pergamon Press, 1991).
- [12] M. V. Berry, N. L. Balazs, M. Tabor, and A. Voros, Ann. Phys. (N.Y.) **122**, 26 (1979).
- [13] M. J. Davis and E. J. Heller, J. Chem. Phys. **75**, 246 (1981).
- [14] J. D. Hanson, E. Ott, and T. M. Antonsen, Phys. Rev. A **29**, 819 (1984).
- [15] O. Bohigas, S. Tomsovic, and D. Ullmo, Phys. Rep. **223**, 43 (1993).
- [16] S. Tomsovic and D. Ullmo, Phys. Rev. E **50**, 145 (1994).
- [17] A. Shudo and K. S. Ikeda, Phys. Rev. Lett. **74**, 682 (1995).
- [18] O. Brodier, P. Schlagheck, and D. Ullmo, Phys. Rev. Lett. **87**, 064101 (2001).
- [19] O. Brodier, P. Schlagheck, and D. Ullmo, Ann. Phys. **300**, 88 (2002).
- [20] M. Sheinman, S. Fishman, I. Guarneri, and L. Rebuzzini, Phys. Rev. A **73**, 052110 (2006).
- [21] A. Bäcker, R. Ketzmerick, S. Löck, and L. Schilling, Phys. Rev. Lett. **100**, 104101 (2008).
- [22] S. Löck, A. Bäcker, R. Ketzmerick, and P. Schlagheck, Phys. Rev. Lett. **104**, 114101 (2010).
- [23] A. Bäcker, R. Ketzmerick, and S. Löck, Phys. Rev. E **82**, 056208 (2010).
- [24] C. Dembowski, H.-D. Gräf, A. Heine, R. Hofferbert, H. Rehfeld, and A. Richter, Phys. Rev. Lett. **84**, 867 (2000).
- [25] D. A. Steck, W. H. Oskay, and M. G. Raizen, Science **293**, 274 (2001).
- [26] W. K. Hensinger, H. Häffner, A. Browaeys, N. R. Heckenberg, K. Helmerson, C. McKenzie, G. J. Milburn, W. D. Phillips, S. L. Rolston, H. Rubinsztein-Dunlop, B. Urcroft, Nature **412**, 52 (2001).
- [27] D. M. Leitner, Phys. Rev. E **48**, 2536 (1993).
- [28] V. A. Podolskiy and E. E. Narimanov, Phys. Lett. **362**, 412 (2007).
- [29] G. Vidmar, H.-J. Stöckmann, M. Robnik, U. Kuhl, R. Höhmann, and S. Grossmann, J. Phys. A **40**, 13883 (2007).
- [30] B. Batistić and M. Robnik, J. Phys. A **43**, 215101 (2010).
- [31] A. Bäcker, R. Ketzmerick, S. Löck, and N. Mertig, Phys. Rev. Lett. **106**, 024101 (2011).
- [32] A. Bäcker, R. Ketzmerick, and A. G. Monastera, Phys. Rev. Lett. **94**, 054102 (2005).
- [33] A. Bäcker, R. Ketzmerick, and A. G. Monastera, Phys. Rev. E **75**, 066204 (2007).
- [34] J. Feist, A. Bäcker, R. Ketzmerick, S. Rotter, B. Huckestein, and J. Burgdörfer, Phys. Rev. Lett. **97**, 116804 (2006).
- [35] A. Ishikawa, A. Tanaka, and A. Shudo, Phys. Rev. Lett. **104**, 224102 (2010).
- [36] F. Haake, *Quantum Signatures of Chaos* (Springer, Berlin, 2001).
- [37] L. Hufnagel, R. Ketzmerick, M.-F. Otto, and H. Schanz, Phys. Rev. Lett. **89**, 154101 (2002).
- [38] H. Schanz, M.-F. Otto, R. Ketzmerick, and T. Dittrich, Phys. Rev. Lett. **87**, 070601 (2001).
- [39] H. Schanz, T. Dittrich, and R. Ketzmerick, Phys. Rev. E **71**, 026228 (2005).
- [40] J. H. Hannay and M. V. Berry, Physica D **1**, 267 (1980).
- [41] S.-J. Chang and K.-J. Shi, Phys. Rev. A **34**, 7 (1986).
- [42] J. P. Keating, F. Mezzadri, and J. M. Robbins, Nonlinearity **12**, 579 (1999).
- [43] L. Bittrich, Ph.D. thesis, Technische Universität Dresden (2010).
- [44] A. Bäcker, L. Bittrich, and R. Ketzmerick, in preparation.
- [45] H. P. Breuer and M. Holthaus, Ann. Phys. **211**, 249 (1991).
- [46] F. M. Izrailev, Phys. Rep. **196**, 299 (1990).
- [47] B. V. Chirikov and D. L. Shepelyansky, Phys. Rev. Lett. **74**, 518 (1995).
- [48] T. Prosen and M. Robnik, J. Phys. A **27**, 8059 (1994).
- [49] A. Bäcker and R. Ketzmerick, unpublished.
- [50] S. Kraut, Diploma thesis, Universität Frankfurt am Main (1996).